

Evaluation of Cuff-Induced Ischemia in the Lower Extremity by Magnetic Resonance Oximetry

Michael C. Langham, PhD,* Thomas F. Floyd, MD,† Emile R. Mohler III, MD,†
Jeremy F. Magland, PhD,* Felix W. Wehrli, PhD*
Philadelphia, Pennsylvania

Objectives

The aim of this study was to evaluate vascular function in the lower extremities by making direct time-course measurement of oxygen saturation in the femoral/popliteal arteries and veins during cuff-induced reactive hyperemia with magnetic resonance imaging-based oximetry.

Background

Magnetic resonance imaging-based oximetry is a new calibration-free technique taking advantage of the paramagnetic nature of blood that depends on the volume fraction of deoxyhemoglobin in red blood cells.

Methods

We compared post-occlusive blood oxygenation time-course of femoral/popliteal vessels in: 1) young healthy subjects (YH) ($n = 10$; mean ankle-brachial index [ABI] 1.0 ± 0.1 , mean age 30 ± 7 years); 2) peripheral arterial disease (PAD) patients ($n = 12$; mean ABI 0.6 ± 0.1 , mean age 71 ± 9 years); and 3) age-matched healthy control subjects (AHC) ($n = 8$; mean ABI 1.1 ± 0.1 , mean age 68 ± 9 years). Blood oxygenation was quantified at 3.0-T field strength with a field mapping pulse sequence yielding the magnetic susceptibility difference between blood in the vessels and surrounding muscle tissue from which the intravascular blood oxygen saturation is computed as %HbO₂.

Results

Significantly longer washout time (42 ± 16 s vs. 14 ± 4 s; $p < 0.0001$) and lower upslope (0.60 ± 0.20 %HbO₂/s vs. 1.32 ± 0.41 %HbO₂/s; $p = 0.0008$) were observed for PAD patients compared with healthy subjects (YH and AHC combined). Furthermore, greater overshoot was observed in YH than in AHC (21 ± 8 %HbO₂ vs. 10 ± 5 %HbO₂; $p = 0.0116$).

Conclusions

Post-occlusive transient changes in venous blood oxygenation might provide a new measure of vascular competence, which was found to be reduced in subjects with abnormal ABI, manifesting in prolonged recovery during the early phase of hyperemia. (J Am Coll Cardiol 2010;55:598–606) © 2010 by the American College of Cardiology Foundation

In the U.S. the number of adults affected by peripheral artery disease (PAD) is as large as 8 million (1), a number expected to rise as the elderly population grows. PAD reduces the quality of life of individuals, but more importantly, the relative risk of cardiovascular events significantly increases. For these reasons, a noninvasive method of detecting early manifestations of atherosclerosis in the lower extremity is desirable. Specifically, a quantitative prognostic tool to identify individuals more susceptible to the major cardiovascular risk factors is desirable, because the Framingham score fails to account for 50% of the mortality and morbidity (2). The initial test used to diagnose PAD is the ankle-brachial index (ABI) measurement, which is calcu-

lated as the ratio between systolic pressures of the ankle and brachial artery. The ABI is simple, inexpensive, painless, reproducible, and can be easily performed in a physician's office. However, the ABI measurement has some limitations, because there is a high specificity but low sensitivity in population-based cohorts (no evidence of pre-existing PAD) (3). In addition, the ABI might be falsely elevated in patients with medial artery calcification. Additional diagnostic tools are needed that provide early assessment of lower extremity PAD before development of flow limiting lesions.

The assessment of vascular function at rest is difficult, because metabolic rate and capillary blood flow in the extremities are not significantly different between PAD and healthy subjects. Even with multiple levels of hemodynamically significant stenoses, nutritive requirements can be maintained via establishment of collateral circulation. However, the high peripheral resistance seen with occlusive PAD cannot accommodate greater transient flow rates induced by

From the Departments of *Radiology and †Medicine, University of Pennsylvania School of Medicine, Philadelphia, Pennsylvania. This work was supported by National Institutes of Health Grants T32 EB000814, R21 HL88182, and RO1 HL 075649.

Manuscript received April 28, 2009; revised manuscript received August 20, 2009, accepted August 30, 2009.

a physiological challenge, such as a cuff-compression or exercise paradigm.

To re-oxygenate hypoxic tissue after a period of ischemia, the blood flow is markedly increased through reduction of microvascular resistance. The resulting increase in shear stress to the endothelium after cuff release leads to vasodilation of the conduit artery mainly via nitric oxide release (4). Thus, reactive hyperemia offers an opportunity to assess microvascular and macrovascular function. Noninvasive imaging modalities that have been used to quantify reactive hyperemia include near-infrared spectroscopy (NIRS) (5–8), single photon emission computed tomography (9), magnetic resonance imaging (MRI) (10,11), and ultrasound (12). Near-infrared spectroscopy and ultrasound are most commonly used, due to their portability. Near-infrared spectroscopy is relatively inexpensive, has excellent temporal resolution, and is less hampered by subject motion. However, the spatial resolution of NIRS is low (on the order of centimeters) and can only provide regional information. The separation of the source-detector probes determines the depth of the layer being probed, and the true path of the infrared light is not known (5). Furthermore, tissue response to the light depends on skin color, body fat, and muscle layers, leading to large intersubject variations and inability to focus on specific vessels or distinguish between arterial and venous saturation. Thus, NIRS allows for the examination of microvascular function in relatively superficial tissues only. Ultrasound measurements of flow-mediated dilation (FMD) in the brachial artery have generated substantial interest in clinical research since its introduction (13). Several studies have since demonstrated the prognostic value of brachial artery FMD (14,15); however, the methodology suffers from substantial inter- and intraobserver variability (e.g., transducer placement) (4,16) and limited spatial resolution. Both effects are magnified, because the relative change of FMD averages <5% (17). Similar to ultrasound, quantitative MRI flow velocimetry can be performed with high spatial and temporal resolution as demonstrated in a recent study in which post-occlusion hyperemia in the femoral artery was evaluated in PAD patients (11).

We evaluated vascular function with a time-course measurement of oxygen saturation in the femoral/popliteal vessels with the aid of a new quantitative magnetic resonance technique that makes use of deoxyhemoglobin's paramagnetism (18). Magnetic resonance imaging oximetry quantifies blood oxygen saturation by spatially mapping the magnetic susceptibility of blood, which scales linearly with $(1 - \text{HbO}_2)$. Blood oxygen saturation is obtained by modeling the vessel as a long paramagnetic cylinder immersed in an external field and relies on the quantification of the induced field of the blood in the vessel relative to surrounding muscle tissue, achieved by measuring the phase of the MR signal. Figure 1 illustrates the basic principles of MR oximetry for quantification of blood oxygen saturation. The feasibility of this approach as well as the method's

accuracy and precision have recently been demonstrated, in phantoms and in vivo in the authors' laboratory (19–21). The present study extends the technique to quantify blood oxygenation during cuff-induced reactive hyperemia in the femoral/popliteal artery and vein.

We hypothesize that washout time, upslope, and overshoot derived from blood oxygenation time-course will provide a quantitative assessment of the vascular competence during the hyperemic period after cuff-induced ischemia. The washout time refers to the time required to observe oxygen-depleted blood in the tissue to pass through the imaging slice once flow is restored. The upslope is the subsequent re-oxygenation rate, and the overshoot represents the transient increase in venous saturation relative to the baseline value. To test the hypothesis, the aforementioned parameters were derived in a pilot study to determine whether PAD patients, diagnosed on the basis of abnormal ABI, differ from age-matched control subjects (AHC) and whether the latter differ from young healthy subjects (YH). The latter comparison is motivated by the fact that aortic stiffness is known to increase with age (22), and there is growing evidence relating increased pressure pulsatility to reduced peripheral reactive hyperemia (23).

Methods

Patient selection. Three groups of subjects were compared: 1) PAD ($n = 12$, mean ABI 0.6 ± 0.1 , mean age 71 ± 9 years, 3 women); 2) AHC ($n = 8$, mean ABI 1.1 ± 0.1 , mean age 68 ± 9 years, 2 women); and 3) YH ($n = 10$, mean ABI 1.0 ± 0.1 , mean age 30 ± 7 years, 4 women).

Abbreviations and Acronyms

ABI	= ankle-brachial index
AHC	= age-matched control subjects
FMD	= flow-mediated dilation
NIRS	= near-infrared spectroscopy
PAD	= peripheral artery disease
SvO₂	= venous oxygen saturation
YH	= young healthy subjects

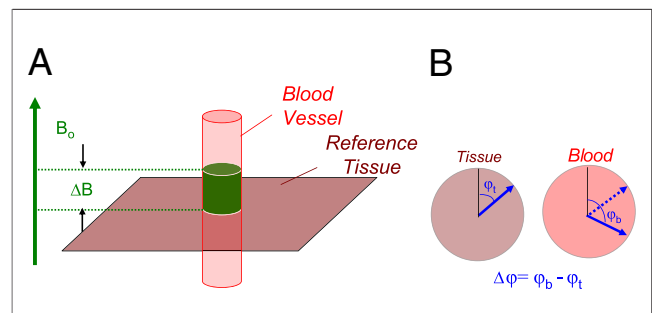


Figure 1 Principle of MR Oximetry

Magnetic resonance (MR) oximetry exploits the small induced field shift caused by the paramagnetic susceptibility of deoxyhemoglobin in blood: (A) field shift ΔB between intravascular blood and surrounding tissue; (B) measurement of the phase of the precessing magnetization in the reference tissue (φ_r), and in the blood (φ_b) a phase difference $\Delta\varphi$ is computed that is proportional to $(1 - \text{HbO}_2)$.

Table 1 Patient Characteristics

	PAD Patients (n = 12)	AHC (n = 8)	YH (n = 10)
Average age, yrs	71 ± 9	68 ± 9	30 ± 7
Male/female, n	9/4	6/2	6/4
Ankle-brachial index	0.6 ± 0.1	1.1 ± 0.1	1.0 ± 0.1
Systolic blood pressure, mm Hg	142 ± 27	128 ± 12	121 ± 18
Diastolic blood pressure, mm Hg	74 ± 7	72 ± 6	68 ± 7

AHC = age-matched control subjects; PAD = peripheral artery disease; YH = young healthy subjects.

Additional patient data are summarized in Table 1. Young healthy subjects (age 20 to 40 years) and AHC were recruited on the basis of their ABI (>0.90 in either leg) and medical history (normotensive and without prior cardiovascular events). The PAD subjects, men and women with a history of PAD, were defined by having ABI <0.80. Patients with a history of myocardial infarction or stroke within 3 months before study enrollment or vascular surgery on the leg selected for scanning were excluded. The ABI of each leg was calculated by dividing the pressure of the dorsalis pedis artery by the higher of the 2 brachial artery blood pressures. Blood pressure was recorded with Doppler ultrasound when the pulse became audible after deflating the cuff at 20 mm Hg above the last audible pulse. Written informed consent was obtained before all examinations after an institutional review board-approved protocol.

Reactive hyperemia in response to cuff-induced ischemia. In preparation for the examinations, subjects were asked to fast for 12 h (except for water), during which period they were also asked to abstain from the following: 1) smoking; 2) taking of vasoactive medications (including over-the-counter medications such as high-dose niacin, decongestants, vitamins C and E); and 3) vigorous physical activity. Ischemia was induced in the lower limb by blood pressure cuff (Aspen Labs A.T.S 1500 Tourniquet System, Aspen Laboratories, Englewood, Colorado) applied on the uppermost part of the thigh to minimize perturbation of the imaging region during cuff inflation or deflation and inflated to 75 mm Hg above systolic pressure but not exceeding 250 mm Hg. Data were collected with 2 different occlusion paradigms of either 3 or 5 min, which were preceded by 2 min of baseline scanning, followed by a 6-min recovery period (Fig. 2). The 2 different paradigms were performed

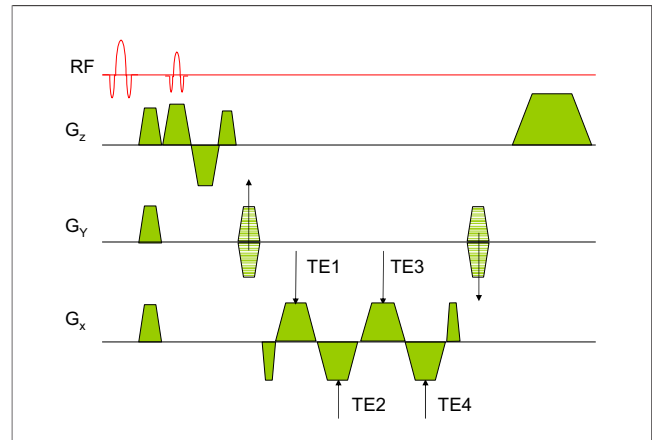


Figure 3 Field-Mapping Pulse Sequence

Spoiled multi-echo gradient-recalled echo pulse sequence. Phase differences are computed from successive equal-polarity echoes (e.g., between echo time TE3 and TE1). MR = magnetic resonance; RF = radiofrequency.

sequentially, with the 5-min cuff occlusion 9 min after deflation of the cuff at the end of the 3-min occlusion period.

MRI protocol. All MR scans were performed on a 3T Siemens Trio scanner with an 8-channel knee array coil (Invivo, Inc., Pewaukee, Wisconsin). Images were acquired with a spoiled multi-echo gradient-recalled echo pulse sequence (Fig. 3) that was programmed with SequenceTree version 3.1 (24). The pulse sequence included fat suppression and flow compensation along the slice direction. Axial images of the lower thigh (approximately 10 cm distal to the boundary of the cuff) were acquired with the following parameters: voxel size and resolution = $1 \times 1 \times 5 \text{ mm}^3$, field of view = $128 \times 128 \text{ mm}^2$, bandwidth = 488 Hz/pixel, 4 echoes (echo time 1 = 4.5 ms), echo spacing of 2.32 ms, temporal resolution of 5, 10, or 20 s achieved with repetition time (TR) = 39, 78, or 156 ms and radiofrequency pulse flip angles = 13° , 19° , or 26° , respectively. Baseline scanning was performed with TR of 156 ms (20-s temporal resolution), subsequently switched to 78 ms (10-s resolution) during cuff occlusion (Fig. 2). The TR was lowered further to 39 ms approximately 10 s before and the first 120 s after cuff deflation to capture the rapid transient changes during hyperemia, providing a temporal resolution

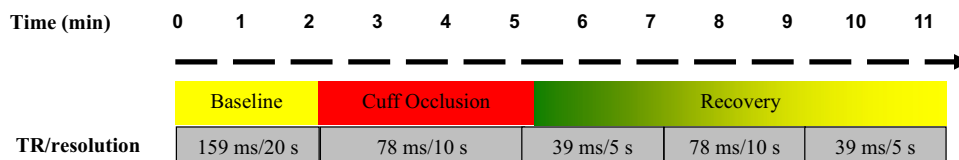


Figure 2 Cuff Paradigm

Three-minute cuff paradigm time line, as an example, is shown with pulse repetition time (TR) and temporal resolution.

of 5 s. During the remaining recovery period, data were collected first at 10-s and subsequently at 20-s temporal resolution. In this manner data size could be minimized during this relatively quiescent period without risking loss of essential information. Before execution of the cuff-inflation paradigm, 20 contiguous scout images were collected at the same spatial resolution but under conditions ensuring maximum vessel visibility (i.e., at high flip angle to maximize flow-related enhancement) for location of the optimum slice as well as to estimate vessel tilt angle (21).

Data analysis. The raw k-space data were saved and processed offline. From the 4 complex images (each being associated with an echo in the pulse sequence of Fig. 3), 2 phase difference images were constructed (25), and the phase from each pixel averaged to yield:

$$\Delta\varphi_{map} = [\arg(Z_3Z_1^*) + \arg(Z_4Z_2^*)] / 2 \quad [\text{Equation 1}]$$

where Z_i represents complex value of a particular pixel from the image of the “i”-th echo and the asterisk denotes complex conjugate. The most significant source of error results from low-frequency modulations of static magnetic field produced by the interface between air and tissue or between adjacent tissue types. The slowly varying modulation was fit to a second-order polynomial (20) and subtracted from $\Delta\varphi_{map}$ before measuring the phase difference between the intravascular phase and average phase of nearby tissue region (Fig. 1). The absolute %HbO₂ in both vein and artery then was computed with

$$\%HbO_2 = \left[1 - \frac{2|\Delta\varphi|/\Delta TE}{\gamma\Delta\chi_{do}Hct \cdot B_0(\cos^2\theta - 1/3)} \right] \times 100 \quad [\text{Equation 2}]$$

where $\Delta\varphi$ is the average intravascular phase relative to surrounding tissue, ΔTE is the echo spacing between the equal-polarity echoes, γ is the gyromagnetic ratio of water protons, $\Delta\chi_{do} = 4\pi \cdot (0.24 \pm 0.02) ppm$ (26) is the susceptibility difference between fully deoxygenated and fully oxygenated erythrocytes, and θ is the vessel tilt angle relative to the main field B_0 . Because the femoral and popliteal vessels are not exactly parallel to B_0 , the local vessel tilt was measured from the scout images from the coordinates of the vessel’s centroid in slices separated by approximately 3 cm. Hematocrit (Hct) was determined from a sample of blood drawn from each subject, in the institution’s Clinical and Translational Research Center.

To quantify vascular competence during reactive hyperemia washout time, upslope and overshoot (defined in Fig. 4) were derived from the venous oxygenation time-course. The washout time refers to the time required for the deoxygenated blood from the hypoxic tissue to reach the scan location, the upslope is the re-oxygenation rate, and the overshoot is the peak venous saturation during hyperemia relative to the average baseline value. Results of upslope, washout, and

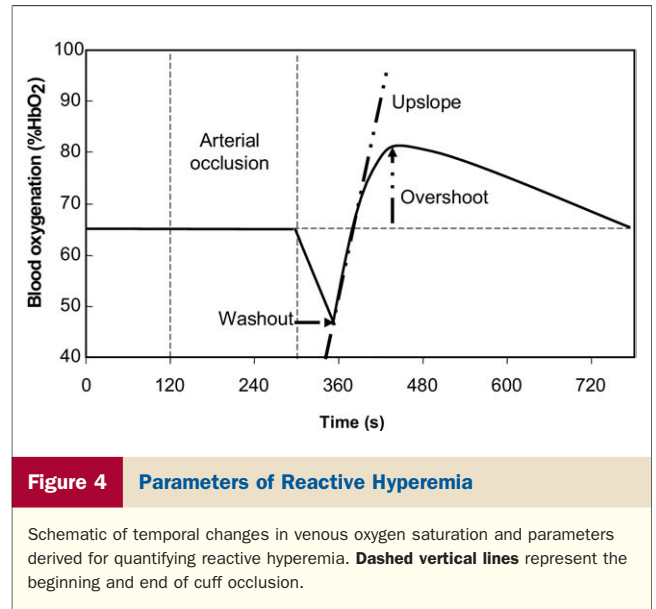


Figure 4 Parameters of Reactive Hyperemia

Schematic of temporal changes in venous oxygen saturation and parameters derived for quantifying reactive hyperemia. Dashed vertical lines represent the beginning and end of cuff occlusion.

overshoot were analyzed (JMP 7.0, SAS Institute, Cary, North Carolina) to determine statistical significance between groups with a Kruskal-Wallis test (nonparametric 1-way analysis of variance) ($p < 0.05$). For simplicity, we performed pair-wise post hoc Wilcoxon tests to evaluate group differences but with a more stringent significance criterion of $p < 0.025$.

Accuracy and precision of MR oximetry has previously been investigated by some of the present authors (21). In phantoms, the effect of vessel noncircularity was found to be negligible for tilt angles $<30^\circ$, in agreement with the theory, and the coefficient of variation in repeat measurements was $<2\%$, achieved with tilt correction alone. In vivo, repeated measurements of %HbO₂ in the femoral vessels performed at multiple levels (where vessel segments differed in geometry such as eccentricity and tilt angle) yielded an average coefficient of variation from 3 subjects of $<5\%$.

Results

Representative magnitude and phase difference images (after correction for regional field inhomogeneity) are shown in Figure 5. Greater phase (corresponding to lower oxygen saturation) in the femoral vein is seen compared with the artery. The phase contrast between artery and surrounding reference tissue is virtually imperceptible, as expected, because muscle tissue and fully oxygenated blood have approximately equal magnetic susceptibility. The average baseline %HbO₂ values of venous and arterial oxygenation for all non-PAD subjects were $64 \pm 8\%$ and $95 \pm 3\%$, respectively, and did not differ significantly from those of PAD patients, $67 \pm 9\%$ and $94 \pm 4\%$. These observations are not surprising, because it is well known that the oxygenation levels at rest do not differ between healthy subjects and PAD patients. This is also in agreement with near-infrared muscle oxygenation studies (8,27).

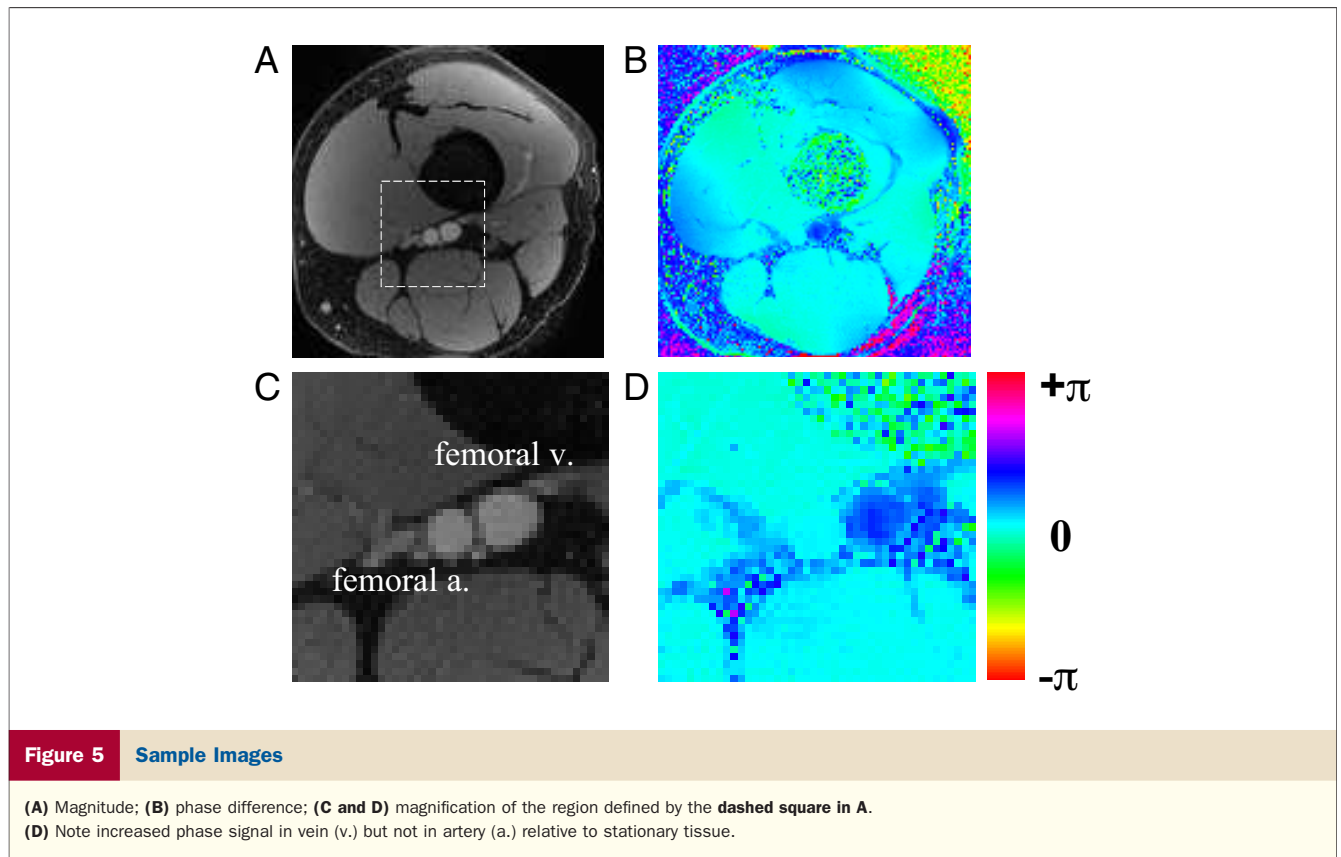


Figure 6 shows the time course of arterial and venous oxygen saturation (S_vO_2) in 3 representative subjects (1 from each group), before, during, and after cuff-induced ischemia. The average values of the washout time, upslope, and overshoot for each group are summarized in Table 2. The overshoot after 5-min occlusion was the only quantity that was significantly different between YH and AHC (21 ± 8 %HbO₂ vs. 10 ± 5 %HbO₂; $p = 0.0116$). On the basis of this result, YH and AHC were combined as a “healthy” group (Table 2, column 4) who were compared with PAD subjects. The latter were characterized by significantly longer washout time and smaller upslope, after both 3- and 5-min cuff occlusions, when compared with subjects with normal ABI. After 5 min of cuff-compression, the average washout time for PAD subjects was 42 ± 16 s compared with 14 ± 4 s ($p < 0.0001$) for healthy subjects. Washout time in PAD subjects varied widely ($SD \pm 16$ s), reflecting the complexity of PAD, in contrast to healthy subjects where this parameter was narrowly distributed ($SD \pm 4$ s). Finally, the average upslope in the normal group was more than twice that of those with PAD (1.32 ± 0.41 %HbO₂/s vs. 0.60 ± 0.20 %HbO₂/s; $p = 0.0008$).

Arterial blood oxygenation was found to remain essentially unchanged during the entire time course, because no oxygen is extracted from the artery at the location of measurement (oxygen extraction takes place in the capillary bed). By contrast, disruption of arterial supply during cuff occlusion is expected to result in gradual depletion of the

tissue oxygen stores. Therefore, upon cuff deflation there is rapid drainage of the oxygen-depleted capillary blood, resulting in a large transient reduction in venous saturation ($\%S_vO_2$) at the observation point, a phenomenon observed in all subjects. This short post-occlusion dip is followed by above-baseline saturation from transient increase in blood flow and subsequent gradual decrease toward baseline values after S_vO_2 has reached a broad maximum. The large difference in minimum venous saturation between YH and AHC shown in Figure 6 is not a consistent finding. The average relative difference in venous saturation with respect to the baseline value $(\Delta S_vO_2)_{\max}$ did not differ (18 ± 8 %HbO₂ vs. 19 ± 9 %HbO₂) between the 2 groups.

Discussion

Blood oxygen saturation is an important physiological parameter that can provide valuable information on a variety of clinical conditions, including congenital heart defects associated with arterial-venous mixing; hypoxemic conditions; and ischemic diseases affecting various organs, such as the heart, brain, kidneys, and gut. In this study, we used oxygen saturation as an endogenous tracer to evaluate peripheral vascular function. A cuff-induced ischemic paradigm was used to assess peripheral arterial disease, because normal blood oxygenation as well as nutritive need can be maintained at rest even in the presence of multiple levels of stenoses through collateral circulation (28). We examined

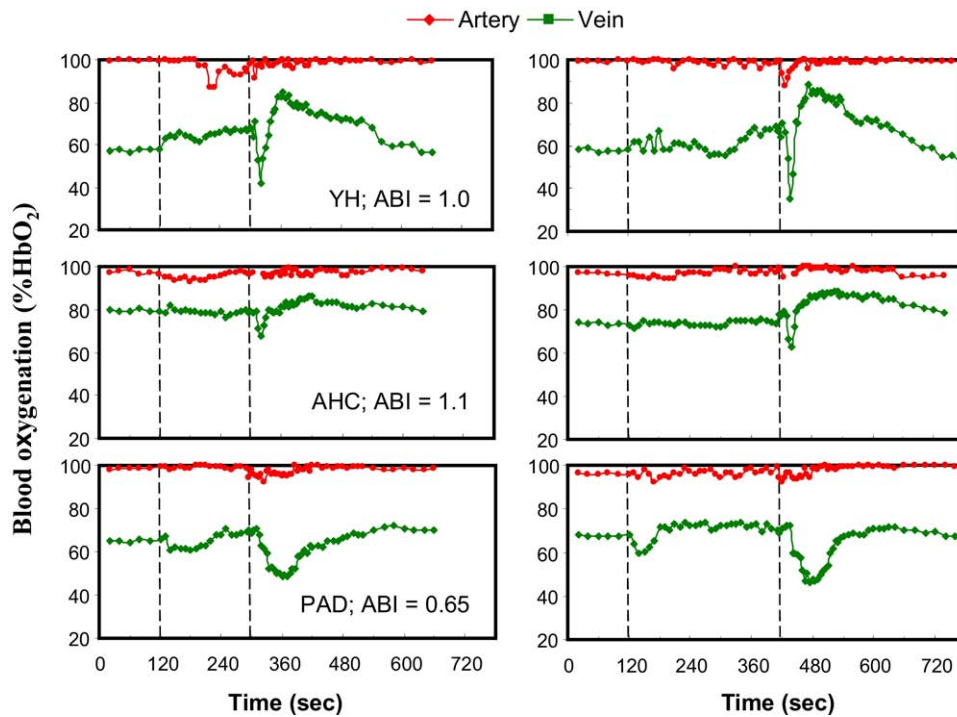


Figure 6 Representative Time-Course of the Blood Oxygenation

For each group a sample 3- (left panel) and 5-min (right panel) cuff occlusion time-course is shown. ABI = ankle-brachial index; AHC = age-matched control subjects; PAD = peripheral artery disease patients; YH = young healthy subjects.

the hypothesis that the rate at which blood in hypoxic tissue is replaced reflects vascular competency. Support for this hypothesis has been provided with the distinguishing behavior of the temporal changes in S_vO_2 between PAD subjects and AHC, with a quantitative magnetic resonance technique dubbed “MR oximetry.” From the time-course, 3 parameters characterizing different temporal phases of reactivity were derived: washout time, upslope, and overshoot.

Most prior studies examining the effect of occlusion-induced ischemia and its hyperemic response used measurement of blood flow and FMD in the conduit vessels with ultrasonography or oxygenation and perfusion in tissue with

NIRS. In the present study, we used a novel method to “label” the blood in the capillary bed via cuff occlusion and followed the fate of the oxygen-depleted blood upon restoration of flow and its subsequent replacement by monitoring the temporal changes in oxygen saturation in the femoral vein. The results reveal that at least 2 of the derived quantities—washout time and upslope—differ significantly between healthy subjects (YH and AHC combined) and those with PAD (Table 2) but do not seem to depend on the duration of cuff occlusion. Neither washout time nor upslope differed significantly between the 2 healthy subject groups. However, the difference in the post-ischemic over-

Table 2 Summary of Study Results

	YH	AHC	Healthy	PAD Patients
3-min occlusion				
Washout (s)	17 ± 7	13 ± 3	17 ± 5	42 ± 15*
Upslope (%HbO ₂ /s)	0.94 ± 0.45	0.92 ± 0.37	0.93 ± 0.41	0.40 ± 0.41*
Overshoot (Δ% S_vO_2)	16 ± 9	9 ± 8	12 ± 9	9 ± 9
5-min occlusion				
Washout (s)	13 ± 4	15 ± 3	14 ± 4	42 ± 16*
Upslope (%HbO ₂ /s)	1.26 ± 0.42	1.41 ± 0.41	1.32 ± 0.41	0.60 ± 0.20*
Overshoot (Δ% S_vO_2)	21 ± 8	10 ± 5†	15 ± 8	12 ± 5

Data are presented as mean ± SD. Column labeled “Healthy” represents averages of YH and AHC. *Significantly different from Healthy; 3 min: washout time $p < 0.0001$; upslope $p < 0.005$; 5 min: washout time $p < 0.0001$; upslope $p = 0.0008$. †Substantial difference from YH; 5 min overshoot $p = 0.0116$.

Abbreviations as in Table 1.

shoot of S_vO_2 was significant between YH and AHC ($21 \pm 8\% \text{HbO}_2$ vs. $10 \pm 5\% \text{HbO}_2$; $p = 0.0116$) after 5-min occlusion but not after 3-min occlusion ($16 \pm 9\% \text{HbO}_2$ vs. $9 \pm 8\% \text{HbO}_2$; $p < 0.16$). Nishiyama et al. (29) found that the peak post-ischemic blood flow rate in the popliteal artery occurs <10 s after 5 min of occlusion, regardless of age in healthy subjects, but the magnitude was significantly greater in young compared with old subjects (average age of 26 vs. 72 years), and the noticeable difference in the flow rate was maintained for approximately 1 min. In a study by Abramson et al. (30), the flow rate in the forearm of healthy young subjects was evaluated in response to 2.5- and 5-min cuff occlusion. The authors found the longer period of tissue hypoxia in the forearm to lead to increased duration of hyperemia as described in the preceding text, and the magnitude of the peak flow—which occurred within 10 to 15 s—increased only marginally after a 5-min occlusion compared with 3 min. A direct comparison cannot be made between our data and the results of Nishiyama et al. (29) and Abramson et al. (30), because we are quantifying venous blood oxygenation instead of arterial blood flow rate. However, it is intuitive that the washout time and upslope—parameters that characterize the early phase of hyperemia—are most likely related to the magnitude and time required to achieve peak post-ischemic flow rate.

A common finding among healthy subjects studied is that the early phase of hyperemia is rather brief (i.e., the blood flow rate reaches its peak and then falls down to one-half the value within approximately 20 s) (29). This is essentially the time we find in our study for oxygen-depleted blood to reach the imaging region. This explains comparable washout time and upslope among the healthy subjects. Nevertheless, it is conceivable that washout time and upslope are both shorter and greater, respectively, in YH but that the difference is too small to be detected with 5-s temporal resolution. Similarly, the observation that a longer occlusion period did not cause increased $(\Delta S_vO_2)_{\max}$ did not differ ($18 \pm 8\% \text{HbO}_2$ vs. $19 \pm 9\% \text{HbO}_2$) among healthy subjects might also reflect the limited temporal resolution.

Finally, the overshoot depends on the blood flow rate, because at higher flow rate the tissue has less time to extract oxygen. Nishiyama et al. (29) found the blood flow rate during the recovery period to be much greater in YH, and according to the work by Abramson et al. (30), it is maintained longer in proportion to the cuff-occlusion period. Similarly, we found a greater overshoot in the younger compared with the older healthy age group, an effect that was significant for 5 min ($p = 0.0116$) but not for 3 min of occlusion ($p < 0.16$). The age-related reduction overshoot might reflect decline in microvascular function associated with age (31).

The upslope, washout, and overshoot in PAD subjects did not seem to depend on the duration of the ischemic period. The effect of PAD on vascular reactivity is complex and not fully understood currently. The combination of microvessel stiffness, collateral circulation, change in endo-

thelial function (nitric oxide release) (32), and possibly reduced capillary density (which might occur from chronic ischemia among more serious cases of PAD) might result in “critical damping” of reactive hyperemia, so that longer cuff-compression does not lead to an observable difference in vascular reactivity. The severity of PAD can be classified in terms of 3 types of vascular reactivity (28) responses after exercise-induced ischemia. In the type-I response the peak blood flow is attained within the first 2 min, but the recovery is significantly delayed. Patients showing such a response are characterized by an extensive network of collateral circulation with a single level of stenosis. In terms of blood oxygenation time-course, we project that these patients would exhibit a relatively short washout time and large upslope among PAD patients but shorter-lasting hyperemia. The type-II response is found in patients with stenoses at 2 levels and, although the post-occlusive blood flow is elevated compared with baseline, the peak flow rate is significantly delayed. This would correspond to longer washout time and lower upslope. Due to markedly shortened hyperemia or delayed peak blood flow, the overshoot might not offer additional information among PAD patients. Finally, patients with severe PAD exhibit abnormal flow patterns that include loss of pulsatility and significantly reduced peak blood flow (33), and in some cases, normal nutritive need cannot be maintained even at rest. None of the PAD subjects in this study belonged to the type-III group, and no attempt was made to classify the patients’ hyperemic response in terms of the types described in the preceding text, because information regarding the severity of PAD was not collected for this pilot study. Although we did not measure arterial flow, post-occlusive flow rate was related to washout time and might thus explain why we observed a larger range of washout times among PAD patients compared with YH and AHC (Table 2).

In the present study cuff-compression was chosen over an exercise paradigm for the same reasons stated in the work by Lederman et al. (10). Cuff-induced ischemia is straightforward to implement, and the examination can be done with the patient immobilized as in a conventional MRI study. Furthermore, reactive hyperemia is induced over the entire lower extremity instead of a specific muscle group. Targeting a specific muscle group might be advantageous if the exact location of the stenosis is known but requires patient compliance, which can affect intra- and intersubject reproducibility. The femoral/popliteal vessel group was chosen over the brachial artery (which has been studied extensively with similar paradigms) (34,35), because PAD predominantly occurs in the lower extremity (36) and might translate to greater sensitivity in assessing disease—in particular, possible evaluation of the early stages of atherosclerosis, the ultimate goal of a vascular prognostic tool. In the work of Nishiyama et al. (29) significantly greater attenuation in FMD was observed in the popliteal than in the brachial artery in older healthy subjects (71% vs. 38%). When FMD was normalized to shear stress, significant attenuation was

no longer observed in the brachial artery (i.e., FMD measurements in the brachial artery might falsely signal vascular dysfunction).

Currently, the differential clinical utility of macro- versus microvascular functional assessment is not fully understood, and further studies are required. Recent work by Dhindsa et al. (37) suggests only modest correlation between micro- and macrovascular parameters in healthy subjects (ages 19 to 68 years). However, among stable patients with advanced peripheral vascular disease, macrovascular function was a stronger indicator for predicting cardiovascular events (38). In contrast, findings by Mitchell et al. (39) indicate a stronger association between cardiovascular risk factors and shear stress or hyperemic velocity, the latter being a measure of microvascular function. On the basis of the respective study cohorts of Huang et al. (38) and Mitchell et al. (39), it has been conjectured that macrovascular function (e.g., FMD) is more sensitive to overt cardiovascular disease, whereas evaluation of microvascular function might be more appropriate for assessment of early stages of atherosclerosis (40) (e.g., age-related effects in healthy subjects as observed by Nishiyama et al. [29]).

In this pilot study, only a limited number of subjects were recruited, and no angiographic assessment of macrovascular architecture was performed to locate the sites of stenoses and collateral circulation in patients with PAD. Additional physiologic measurements such as quantification of the time-course of the blood flow rate (11,41) during the hyperemic response as well as a systemic assessment of arterial compliance as a part of single integrated examination might provide a more detailed vascular assessment among subjects at risk but without symptoms of PAD. Magnetic resonance imaging in the form of MR angiography has been used routinely for at least a decade in the clinic (having virtually supplanted plain-film angiography) for grading of stenoses and assessment of collateralization (42). However, as a functional tool, MRI is still in the realm of research—such as for quantifying tissue perfusion (43,44). Our study results show MR technology has potential to provide, in a single session, both structural and physiologic parameters to aid in assessing PAD.

Acknowledgment

The authors thank Helen Peachey for her excellent work in research coordination.

Reprint requests and correspondence: Dr. Felix W. Wehrli, 1 Founders, University of Pennsylvania Medical Center, 3400 Spruce Street, Philadelphia, Pennsylvania 19104. E-mail: wehrli@mail.med.upenn.edu.

REFERENCES

1. Hirsch AT, Murphy TP, Lovell MB, et al. Gaps in public knowledge of peripheral arterial disease: the first national PAD public awareness survey. *Circulation* 2007;116:2086–94.
2. Minson CT, Green DJ. Measures of vascular reactivity: prognostic crystal ball or Pandora's box? *J Appl Physiol* 2008;105:398–9.
3. Doobay AV, Anand SS. Sensitivity and specificity of the ankle-brachial index to predict future cardiovascular outcomes: a systematic review. *Arterioscler Thromb Vasc Biol* 2005;25:1463–9.
4. Widlansky ME, Gokce N, Keaney JF Jr., Vita JA. The clinical implications of endothelial dysfunction. *J Am Coll Cardiol* 2003;42:1149–60.
5. Boushel R, Piantadosi CA. Near-infrared spectroscopy for monitoring muscle oxygenation. *Acta Physiol Scand* 2000;168:615–22.
6. Kragelj R, Jarm T, Erjavec T, Presern-Strukelj M, Miklavcic D. Parameters of postocclusive reactive hyperemia measured by near infrared spectroscopy in patients with peripheral vascular disease and in healthy volunteers. *Ann Biomed Eng* 2001;29:311–20.
7. Yu G, Durduran T, Lech G, et al. Time-dependent blood flow and oxygenation in human skeletal muscles measured with noninvasive near-infrared diffuse optical spectroscopies. *J Biomed Opt* 2005;10:024027.
8. Franceschini M, Fantini S, Palumbo R, et al. Quantitative near-infrared spectroscopy on patients with peripheral vascular disease. In: Benaron DA, Chance B, Ferrari M, editors. *Proc SPIE*. San Diego, CA: SPIE, 1997:112–5.
9. Dupuis J, Arsenault A, Meloche B, Harel F, Staniloae C, Gregoire J. Quantitative hyperemic reactivity in opposed limbs during myocardial perfusion imaging: a new marker of coronary artery disease. *J Am Coll Cardiol* 2004;44:1473–7.
10. Ledermann HP, Schulte AC, Heidecker HG, et al. Blood oxygenation level-dependent magnetic resonance imaging of the skeletal muscle in patients with peripheral arterial occlusive disease. *Circulation* 2006;113:2929–35.
11. Schwitler J, Oelhafen M, Wyss BM, et al. 2D-spatially-selective real-time magnetic resonance imaging for the assessment of microvascular function and its relation to the cardiovascular risk profile. *J Cardiovasc Magn Reson* 2006;8:759–69.
12. Corretti MC, Anderson TJ, Benjamin EJ, et al. Guidelines for the ultrasound assessment of endothelial-dependent flow-mediated vasodilation of the brachial artery: a report of the International Brachial Artery Reactivity Task Force. *J Am Coll Cardiol* 2002;39:257–65.
13. Celermajer DS, Sorensen KE, Gooch VM, et al. Non-invasive detection of endothelial dysfunction in children and adults at risk of atherosclerosis. *Lancet* 1992;340:1111–5.
14. Karatzis EN, Ikonomidis I, Vamvakou GD, et al. Long-term prognostic role of flow-mediated dilatation of the brachial artery after acute coronary syndromes without ST elevation. *Am J Cardiol* 2006;98:1424–8.
15. Katz SD, Hryniewicz K, Hriljac I, et al. Vascular endothelial dysfunction and mortality risk in patients with chronic heart failure. *Circulation* 2005;111:310–4.
16. De Roos NM, Bots ML, Schouten EG, Katan MB. Within-subject variability of flow-mediated vasodilation of the brachial artery in healthy men and women: implications for experimental studies. *Ultrasound Med Biol* 2003;29:401–6.
17. Benjamin EJ, Larson MG, Keyes MJ, et al. Clinical correlates and heritability of flow-mediated dilation in the community: the Framingham Heart Study. *Circulation* 2004;109:613–9.
18. Haacke EM, Lai S, Reichenbach JR, et al. In vivo measurement of blood oxygen saturation using magnetic resonance imaging: a direct validation of the blood oxygen level-dependent concept in functional brain imaging. *Hum Brain Mapp* 1997;5:341–6.
19. Fernández-Seara M, Detre JA, Techawiboonwong A, Wehrli FW. MR susceptometry for measuring global brain oxygen extraction. *Magn Reson Med* 2006;55:967–73.
20. Langham MC, Magland JF, Floyd TF, Wehrli FW. Retrospective correction for induced magnetic field inhomogeneity in measurements of large-vessel hemoglobin oxygen saturation by MR susceptometry. *Magn Reson Med* 2009;61:626–33.
21. Langham M, Magland J, Epstein C, Floyd T, Wehrli FW. Accuracy and precision of MR blood oximetry based on the long paramagnetic cylinder approximation of large vessels. *Magn Reson Med* 2009;62:333–40.
22. Vaitkevicius PV, Fleg JL, Engel JH, et al. Effects of age and aerobic capacity on arterial stiffness in healthy adults. *Circulation* 1993;88:1456–62.

23. Mitchell GF. Effects of central arterial aging on the structure and function of the peripheral vasculature: implications for end-organ damage. *J Appl Physiol* 2008;105:1652–60.
24. Magland J, Wehrli FW. Pulse sequence programming in a dynamic visual environment. *Proc Intl Soc Mag Reson Med* 2006;14:578.
25. Bernstein MA, Grgic M, Brosnan TJ, Pelc NJ. Reconstructions of phase contrast, phased array multicoil data. *Magn Reson Med* 1994;32:330–4.
26. Spees WM, Yablonskiy DA, Oswood MC, Ackerman JJ. Water proton MR properties of human blood at 1.5 Tesla: magnetic susceptibility, T(1), T(2), T*(2), and non-Lorentzian signal behavior. *Magn Reson Med* 2001;45:533–42.
27. Comerota AJ, Thom RC, Kelly P, Jaff M. Tissue (muscle) oxygen saturation (StO₂): a new measure of symptomatic lower-extremity arterial disease. *J Vasc Surg* 2003;38:724–9.
28. Strandness DE Jr. Flow dynamics in circulatory pathophysiology. In: Hwang N, Normann, NA, editors. *Cardiovascular Flow Dynamics and Measurements*. Baltimore, MD: University Park Press, 1977: 327–8.
29. Nishiyama SK, Wray DW, Richardson RS. Aging affects vascular structure and function in a limb-specific manner. *J Appl Physiol* 2008;105:1661–70.
30. Abramson DI, Tuck S Jr., Bell Y, Mitchell RE, Zayas AM. Effect of short periods of arterial occlusion on blood flow and oxygen uptake. *J Appl Physiol* 1961;16:851–7.
31. Castelli WP. Epidemiology of coronary heart disease: the Framingham study. *Am J Med* 1984;76:4–12.
32. Moncada S, Higgs A. The L-arginine-nitric oxide pathway. *N Engl J Med* 1993;329:2002–12.
33. Fronck A, Coel M, Berstein EF. Quantitative ultrasonographic studies of lower extremity flow velocities in health and disease. *Circulation* 1976;53:957–60.
34. Utz W, Jordan J, Niendorf T, et al. Blood oxygen level-dependent MRI of tissue oxygenation: relation to endothelium-dependent and endothelium-independent blood flow changes. *Arterioscler Thromb Vasc Biol* 2005;25:1408–13.
35. Stoner L, Sabatier MJ, Black CD, McCully KK. Occasional cigarette smoking chronically affects arterial function. *Ultrasound Med Biol* 2008;34:1885–92.
36. Osika W, Dangardt F, Gronros J, et al. Increasing peripheral artery intima thickness from childhood to seniority. *Arterioscler Thromb Vasc Biol* 2007;27:671–6.
37. Dhindsa M, Sommerlad SM, DeVan AE, et al. Interrelationships among noninvasive measures of postischemic macro- and microvascular reactivity. *J Appl Physiol* 2008;105:427–32.
38. Huang AL, Silver AE, Shvenke E, et al. Predictive value of reactive hyperemia for cardiovascular events in patients with peripheral arterial disease undergoing vascular surgery. *Arterioscler Thromb Vasc Biol* 2007;27:2113–9.
39. Mitchell GF, Parise H, Vita JA, et al. Local shear stress and brachial artery flow-mediated dilation: the Framingham Heart Study. *Hypertension* 2004;44:134–9.
40. Philpott A, Anderson TJ. Reactive hyperemia and cardiovascular risk. *Arterioscler Thromb Vasc Biol* 2007;27:2065–7.
41. Oelhafen M, Schwitter J, Kozerke S, Luechinger R, Boesiger P. Assessing arterial blood flow and vessel area variations using real-time zonal phase-contrast MRI. *J Magn Reson Imaging* 2006;23:422–9.
42. Miyazaki M, Lee VS. Nonenhanced MR angiography. *Radiology* 2008;248:20–43.
43. Carlier PG, Bertoldi D, Baligand C, Wary C, Fromes Y. Muscle blood flow and oxygenation measured by NMR imaging and spectroscopy. *NMR Biomed* 2006;19:954–67.
44. Wu WC, Wang J, Detre JA, Ratcliffe SJ, Floyd TF. Transit delay and flow quantification in muscle with continuous arterial spin labeling perfusion-MRI. *J Magn Reson Imaging* 2008;28:445–52.

Key Words: blood oxygen saturation ■ magnetic resonance oximetry ■ peripheral arterial disease ■ phase image ■ reactive hyperemia.